

FINAL TECHNICAL REPORT

November, 2011

Grant Award Numbers: G10AP00020 and G10AP00021

Improving Three-dimensional Seismic Velocity Models and Earthquake Locations for Puerto Rico and the U.S. Virgin Islands: Collaborative Research between University of Miami and University of Puerto Rico in Mayagüez

Guoqing Lin

Division of Marine Geology and Geophysics
Rosenstiel School of Marine and
Atmospheric Science
University of Miami
4600 Rickenbacker Cswy
Miami, FL 33149

Email: glin@rsmas.miami.edu

Victor A. Huérfano

Puerto Rico Seismic Network
Department of Geology
University of Puerto Rico, Mayaguez
PO Box 9017
Mayaguez PR 00681

victor@prn.uprm.edu

ABSTRACT

The island of Puerto Rico has a long history of damaging earthquakes. Major earthquakes from off-shore sources have affected Puerto Rico in 1520, 1615, 1670, 1751, 1787, 1867, and 1918 (Mueller et al, 2003; PRSN Catalogue). Recent trenching has also yielded evidence of possible M7.0 events inland (Prentice and Mann, 2005). The high seismic hazard, large population, high tsunami potential and relatively poor construction practice can result in a potentially devastating combination. Efficient emergency response in the event of a large earthquake will be crucial to minimizing the loss of life and disruption of lifeline systems in Puerto Rico and facilitate a faster recovery.

The Puerto Rico Seismic Network (PRSN) currently operates 25 seismic sites distributed among the islands of Puerto Rico, the Virgin Islands and the eastern portion of the Dominican Republic (Figure 1). All of the seismic activity occurring within latitudes 17.0°N to 20°N and -63.5°E to -69°E; are processed and located by the PRSN staff. Results of this analysis is routinely distributed to a variety of national and local agencies including national and regional networks, as well as emergency management agencies in Puerto Rico in the eventuality of a significant earthquake. The current instrumentation allows earthquake detection with $M_d > 2.8$ (Mendoza and Huérfino, 2005) locally (within its Area of Responsibility or AOR) and moderate events in the Caribbean region. Earthquakes felt in Puerto Rico beyond its AOR are also routinely processed and shared among regional networks and general public. All seismic data of a subset of PRSN stations are exported in real-time to USGS, US tsunami warning centers and other regional networks as well as to IRIS DMC.

The current crustal structure used in the daily operations by the PRSN consists of four horizontal layers over a mantle half space with a constant V_p/V_s ratio and the degree of uncertainty in the crustal velocities is actually unknown (Huérfino and Bataille, 1994). We analyze the entire micro seismic catalogue currently archived by the PRSN, due to the complexity in the analysis we select a specific set of events to: (1) Identify arrival phase station corrections, (2) relocate and (3) invert to retrieve a 3D velocity model.

The long term goal is to develop high-quality three-dimensional (3D) P- and S-wave velocity models, that resulting method should be used to obtain high-precision earthquake locations in Puerto Rico and the Virgin Islands. Accurate earthquake locations and high-quality 3D seismic velocity models are central for earthquake hazard assessments. 3D velocity models are necessary for determining accurate earthquake locations and focal mechanisms, for developing ground motion models, and for relating seismicity to geologic structures. Earthquake locations are essential for defining fault geometries, assessing seismogenic behavior of faults, and investigating phenomena such as earthquake triggering.

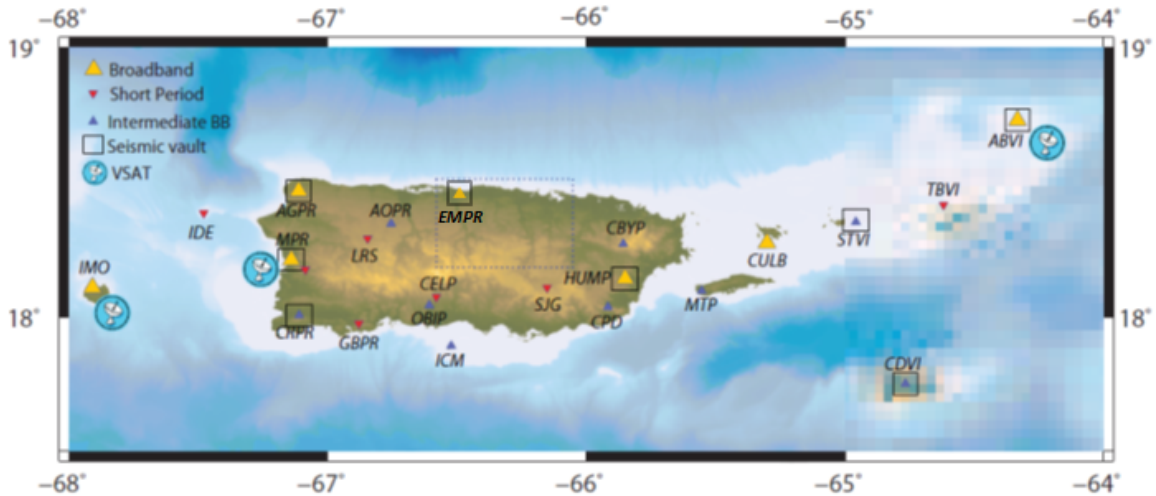


Figure 1: Map of Puerto Rico and the Virgin Islands showing current sensor type in operation at the. Yellow triangles are long period broadband sensors. Blue triangles are intermediate broadband sensors. Inverted triangles are short period instruments. Stations within a black square represent existing seismic vaults. The satellite icon next to a station indicates existing satellite communications up/down-link.

INTRODUCTION

The US Commonwealth of Puerto Rico has a population of 3.8 million (2000 Census, Clinton et al, 2007), which amounts to a higher population density than any US state. The island, approximately 160km from east to west by 50km from north to south, is bounded by off-shore active faults on all sides. Numerous local and regional events in the recorded history with $M > 7.0$ (1670, 1751, 1787), some of which have generated tsunamis (1867 and 1918), have caused extensive damage to local infrastructure; the last significant ground motions were felt on-shore in 1918, the Mona Canyon Event. Recent trenching has also yielded evidence of possible $M 7.0$ events inland (Prentice and Mann, 2000). The USGS hazard maps (Mueller et al, 2003) indicate that the seismic hazard is similar to the Basin and Range province in the Western USA, and the island is assigned Seismic Zone 3. Currently the commonwealth of Puerto Rico is implementing the new IBC. The high seismic hazard, large population, high tsunami potential and relatively poor construction practice can result in a potentially devastating combination. Efficient emergency response in the event of a large earthquake will be crucial to minimizing the loss of life and disruption of lifeline systems in Puerto Rico.

The earthquake and tsunami risk in the north-east Caribbean is also very real. Aside from the potential for large magnitude events (Huérfino, 2003), recent bathymetry studies have shown numerous large landslide scarps and cliffs near the Puerto Rico Trench as well as the Muertos Trough (Grindlay et al., 2005a; Grindlay et al., 2005b; ten Brink, 2004). The off-shore bathymetry is particularly severe to the North of the island, where the Puerto Rico Trench drops to a depth of over 8.3 km just 180 km north of the island. The interior of the island is mountainous; resulting in much of the population being concentrated in the at-risk low-lying coastal flood plains and alluvial basins.

The first step in providing an appropriate response to such a disaster is the knowledge of the real fault systems and the associate potential. A timely knowledge of the magnitude, location and expected ground shaking and damage patterns from the event are vital in terms of response. This requires a modern and dense seismic network, capable not only of recording the earthquake ground motion without saturation, but also doing so in real-time and then providing data for near-immediate analysis, which can be made available to the emergency services and community at large. As a matter of fact, the input parameters used in the location analysis must be realistic and validated via different approaches. The current crustal structure used in the daily operations by the PRSN consists of four horizontal layers over a mantle half space with a constant Vp/Vs ratio and the degree of uncertainty in the crustal velocities is actually unknown.

There are over 20000 events in the catalogue (Figure 2), more than 20 with $M > 5.0$. The largest event was an $M 5.8$, occurring at 120km depth, just beneath of Moca, PR, on 16 May 2010. Shallow seismicity is concentrated in regions along the Mona Canyon, the region between the Puerto Rican Trench and the 19° N fault zone, the Sombrero fault zone, and on-land across the south of Puerto Rico. The oblique subduction of the North American Plate under the Puerto Rican microplate appears to be the source of much of the deep seismicity. The seismicity is dominated by 3 regions; 2 to the North of the island, near the Puerto Rico Trench, and another in the southwest of the island, near Cabo Rojo. Huérfino et al. (2005) suggest the increased seismicity in SW Puerto Rico may be due to local topographic effects.

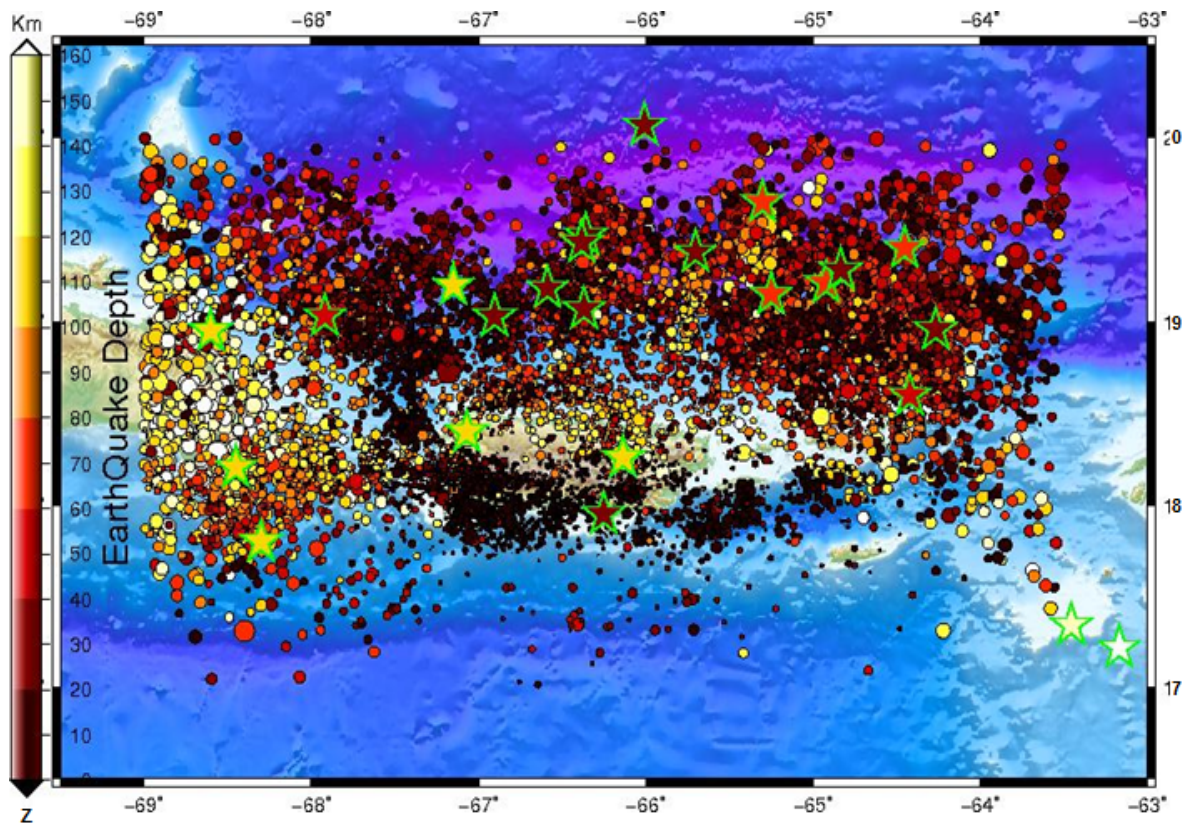


Figure 2: Epicentral map of Puerto Rico and the Virgin Islands showing current microseismic catalogue. Stars represent the location of events with $M \geq 5$.

DATA PROCESING AND RESULTS

Based on the quality (C and up) and magnitude ($M \geq 4$), we performed an AOR (Area of Responsibility) global search, a total of 422 events match the criteria and were used as input for FMTOMO (<http://rses.anu.edu.au/~nick/fmtomo.html>) and 2310 sources were selected to apply the COMPLOC relocation package (<http://www.rsmas.miami.edu/personal/glin/COMPLOC.html>). Depths range from 1 to 140 km. Our initial work was focused on accumulating a comprehensive set of phase arrival picks for use in the FMM (Fast Marching Method) tomographic inversion to perform an initial relocation, simultaneously the COMPLOC method was used to compliment the results. In the second stage, previous relocations were used as input to FFM full inversion to compute a 3D structure. As a previous work, we analyze the full set of data to infer the station corrections.

STATION CORRECTIONS

Station corrections can improve the accuracy of travel-time calculations in case of near-surface deviations of seismic velocities from the applied velocity model. The first step to analyze the PRSN catalogue was to identify the P and S average station corrections (Figure 3), the input data was the raw microseismic catalogue which was compiled using a 4 layers model without lateral velocity variations and the HYPOINVERSE (HYPO2K) location program (Klein, 2002).

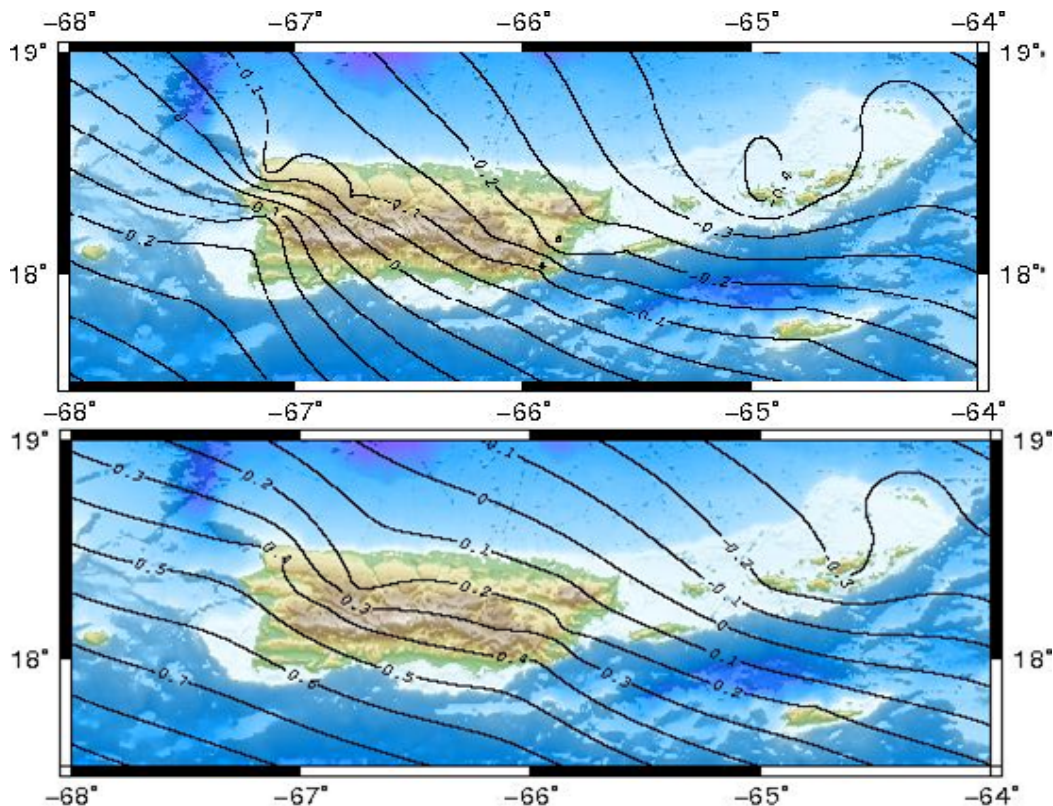


Figure 3. Preliminary station corrections in seconds for P-wave (top) and S-wave (Bottom) phase arrival times for the 1D velocity model displayed as contour lines.

In addition to the difficulties in detecting off-shore events, exact earthquake location is also difficult in the region as most of the stations lie in a band between 18°N and 18.5°N, with poor azimuthal constraint on events lying to the north and south (Mendoza and Huérfino, 2005).

For the computations no any station was selected as the reference station. The station corrections range from -0.4 to +0.3 s for P wave and from -0.5 to 1 s for S wave, and are correlated spatially over a distance of about 10 km. This result could be interpreted as an indication that an improvement of the 1D velocity model should be attempted, especially in the Virgin Islands where the variations are clearly negative for P and S phases or in the western Puerto Rico where stations corrections are positive.

EARTQUAKE RELOCATION

There were two stages: (1) The Fast Marching Schema and (2) The COMLOC method.

1. THE FAST MARCHING SCHEMA

The process of calculating traveltimes to points adjacent to the minimum traveltime point of the narrow band is achieved by solving the Eikonal Equation using finite difference upwind gradient operators which take into account the direction of flow of information.

The Fast Marching Method (FMM) is a narrow band level set method for solving Eikonal-type equations (Sethian J.A, 1999; Rawilson N. 2005, 2006 [a,b],2007,2010). The unconditional stability of the scheme comes from finding entropy-satisfying weak solutions to the Eikonal Equation that permit the formation and propagation of gradient discontinuities in the evolving wavefront. The FMM systematically constructs traveltimes (T) in a downwind fashion from known values upwind by employing a *narrow band* approach (Figure 4). The scheme works by locating the grid point with minimum traveltime within the narrow band of close points. This is achieved by using a heap sorting algorithm; hence the efficiency of the scheme in the presence of M grid points. The minimum traveltime node is then added to the set of alive points. All grid points surrounding the new alive points that are not alive have their value updated (if they are close) or calculated for the first time (if they are far).

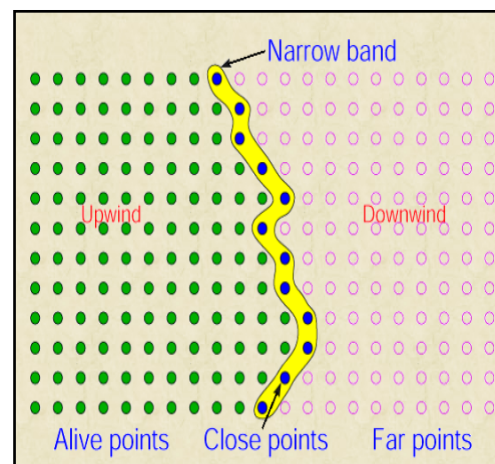


Figure 4. Narrow band method for tracking the first arrival wavefront in continuous media. (from: Rawilson, et al, 2006).

To relocate a data set of sources, the multi-stage FMM need to be solved once for each receiver, with the resulting traveltimes fields stored in look-up tables. Using the principle of traveltimes reciprocity, source-receiver traveltimes at an arbitrary point can be extracted. In complex velocity models with poor initial locations, a fully non-linear or global search algorithm is preferable to an iterative non-linear one. We define initially a rectangular grid of reference nodes about the sources, the traveltimes field is then computed along an expanding wavefront, which means that the computational front may pass from the initial coarse grid back into the finer one. To preserve numerical stability, information only flows out of the refined grid and never back into it. The region of study is bounded by lat: 17.0 – 20N and 63.5-69W, but selected data point were constrained to 17.8 – 18.5N and 65.6 to 67.2W and depths down to 120 km. For synthetics, an array of 10x10 receptors was predefined. The local upper crust 1D model was extended by using the AK135 model.

In average our first attempt to apply FMM indicates very small spatial variation as comparing to the original locations, $DX \approx 10$ km, $DY \approx 1$ km and $DZ \approx 0.1$ km for the complete data set (Figure 5). Once removed scatter points we can see variations of less than a kilometer indicating the original data set provided by PRSN is a high precision catalogue. A major issue is the lack of secondary phases in the catalogue.

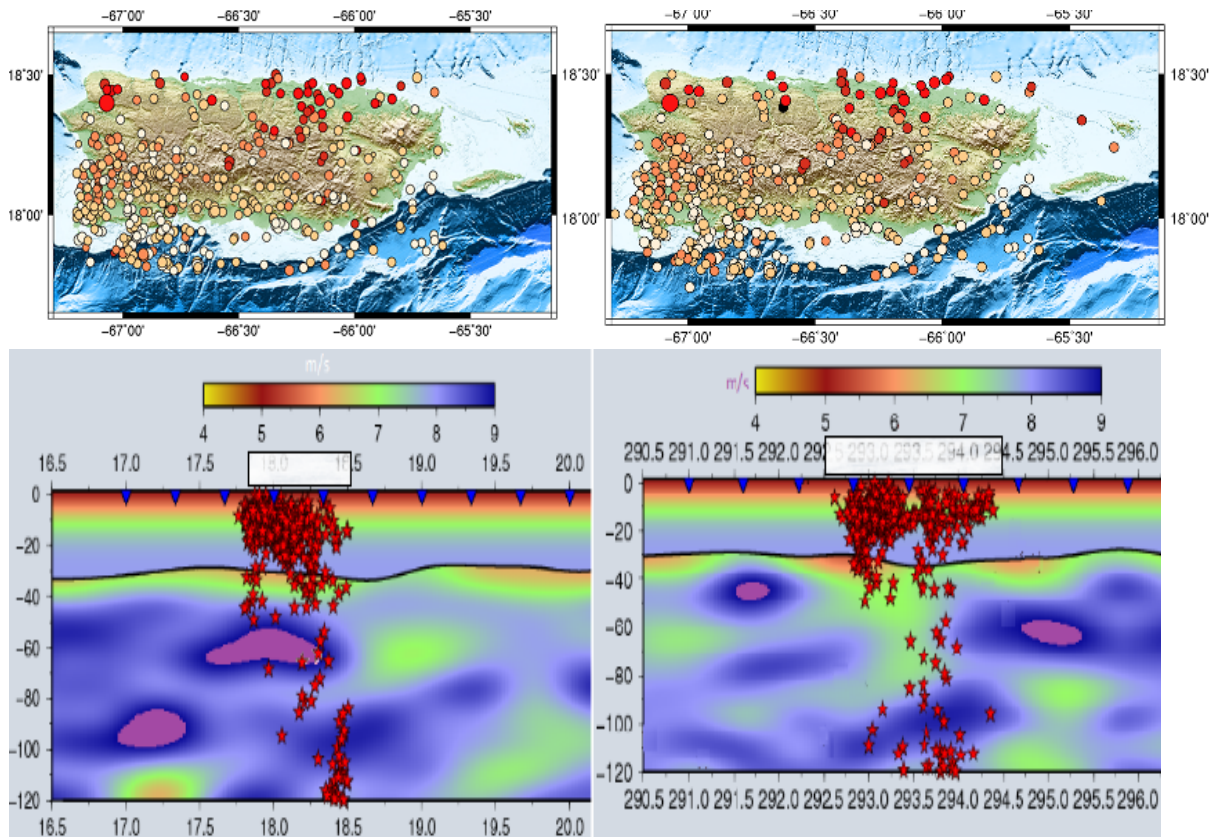


Figure 5. Results from the earthquake relocation process. (Top left) raw catalogue, (top right) relocations. Cross sections are also projected on the (bottom left) S-N and (bottom right) E-W. Note that the horizontal slice at 30 km depth feature velocity discontinuities as a result of the undulating Moho. Red stars denote sources and blue inverted triangles denote receivers. Puerto Rico is represented as a transparent rectangle.

2. THE COMPLOC METHOD

We relocate over 2300 earthquakes between 1986 and 2009 in the crust and upper mantle of the Puerto Rico Island recorded by the Puerto Rico Seismic Network (PRSN), Picks with travel time residuals above 5 sec are removed. Each event has 5 or more P and/or S first-arrivals. The maximum distance from events to stations is set as 100 km to avoid the Pg/Pn ambiguity.

We start with the one-dimensional (1-D) velocity model currently used in the PRSN daily operations and obtain a 1-D “minimum” model by applying the VELEST program. We apply the COMPLOC earthquake location package to improve relative locations by computing the source-specific station terms from arrival time residuals of nearby events. We also compared results using different distance cutoffs to test the reliability of our velocity model. Our results show improvements compared to the PRSN catalog locations. Relative location errors are estimated by perturbing our observations with Gaussian distributed random noises with the standard deviation appropriate for our data.

To invert for a more reliable 1-D P wave velocity model, we used the VELEST program, written in Fortran language by Kissling et al. (1994). The 1-D velocity model used for the PRSN daily operation was adopted as our initial model (shown in Figure 6). 212 master events with at least 9 P picks were used to invert for velocity parameters. Low velocity zone was not allowed during inversion. To calculate the optimizing 1-D model, the numbers of layers and layer thickness, damping parameters are assigned first. The inversion is solved by damped least squared matrix. Because station correction has trade-off with velocity model, we set damping of station corrections as 999. i.e., no station corrections included. After many damping tests, we found out the optimal value for velocity damping was 50 when we followed the guideline of Kissling et al. (1994) to keep initial damping coefficient of 0.01 for the hypocentral parameters, which best optimize the data misfit and model variance. After continuing trial and error procedure, the minimum 1-D model was generated with the root-mean-squares (RMS) of 0.20 and data variance of 0.07, compared to initial model with the RMS of 0.41 and data variance of 0.29. (Figure 6).

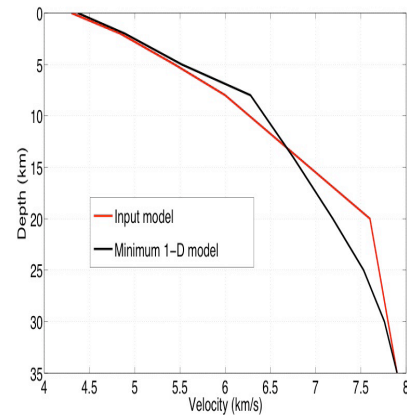


Figure 6. The comparison of the input model and the Minimum velocity model.

A total of 2,310 events recorded during the period of 1986-2009 were relocated using the source-specific station terms (SSST) method (Richards-Dinger and Shearer, 2000; Lin and Shearer, 2005). We chose events using the criteria of at least 5 picks, source-station distance cutoff of 100 km, residual cutoff of 5 sec, and event depths less than 32km. The observed P and S picks were weighted equally. The relocation process was implemented by running the COMPLOC package by Lin and Shearer (2006). The location part and computation of station terms are separated in the COMPLOC. Ten iterations were conducted to compute static station terms and 20 for source-specific station terms (SSST). We applied the shrinking-box SSST approach, which was shown to be able to improve absolute event locations compared with the regular SSST method (Lin and Shearer, 2005). The distribution of epicenters from the PRSN is shown in Figure 7. Among the highly scattered locations, they fall into groups on eastern and southwestern regions. The southwestern high seismicity area is made up of three major serpentinite belts (Huerfano et al., 2005). The earthquakes are concentrated around the three serpentines belts within the Bermeja Complex. The eastern cluster is lower cretaceous layered rocks area. The close-up views of southwestern seismic zone are also shown in Figure 6. The seismicity is more clearly align to Cerro Golden Fault Zone. To show variations in depth distribution, we present cross-sections along two profiles AA' and BB' in Figure 8. The RMS of travel time residuals was reduced from 0.34 s to 0.19 s after the SSST relocation.

To estimate the uncertainties in relative locations, we applied the bootstrap approach (Efron and Gong, 1983). We perturbed the picks with Gaussian random errors at best-fit locations and relocate all the events for 100 times. We calculated the standard deviations of each perturbed relocations in horizontal and vertical direction as relative location uncertainties (Richards-Dinger and Shearer, 2000). The horizontal and vertical location uncertainties with the PRSN 1-D velocity model are 0.07 km and 0.11 km, respectively, and are 0.04 km and 0.07 km with the minimum 1-D model.

In this study, the relocated events show compacter clusters around both the GNPRFZ (Greater Northern Puerto Rico Fault Zone) and GSPRFZ (Greater Southern Puerto Rico Fault Zone) compared to PRSN catalogue. The serpentinite belts correlate with the distribution of event locations in southwestern Puerto Rico Island. New “minimum” 1-D velocity model was developed for the Puerto Rico Island, ensuring more accurate earthquake relocation. Relative location errors were estimated with the horizontal error of 40 m and vertical error of 70 m with the minimum 1-D model.

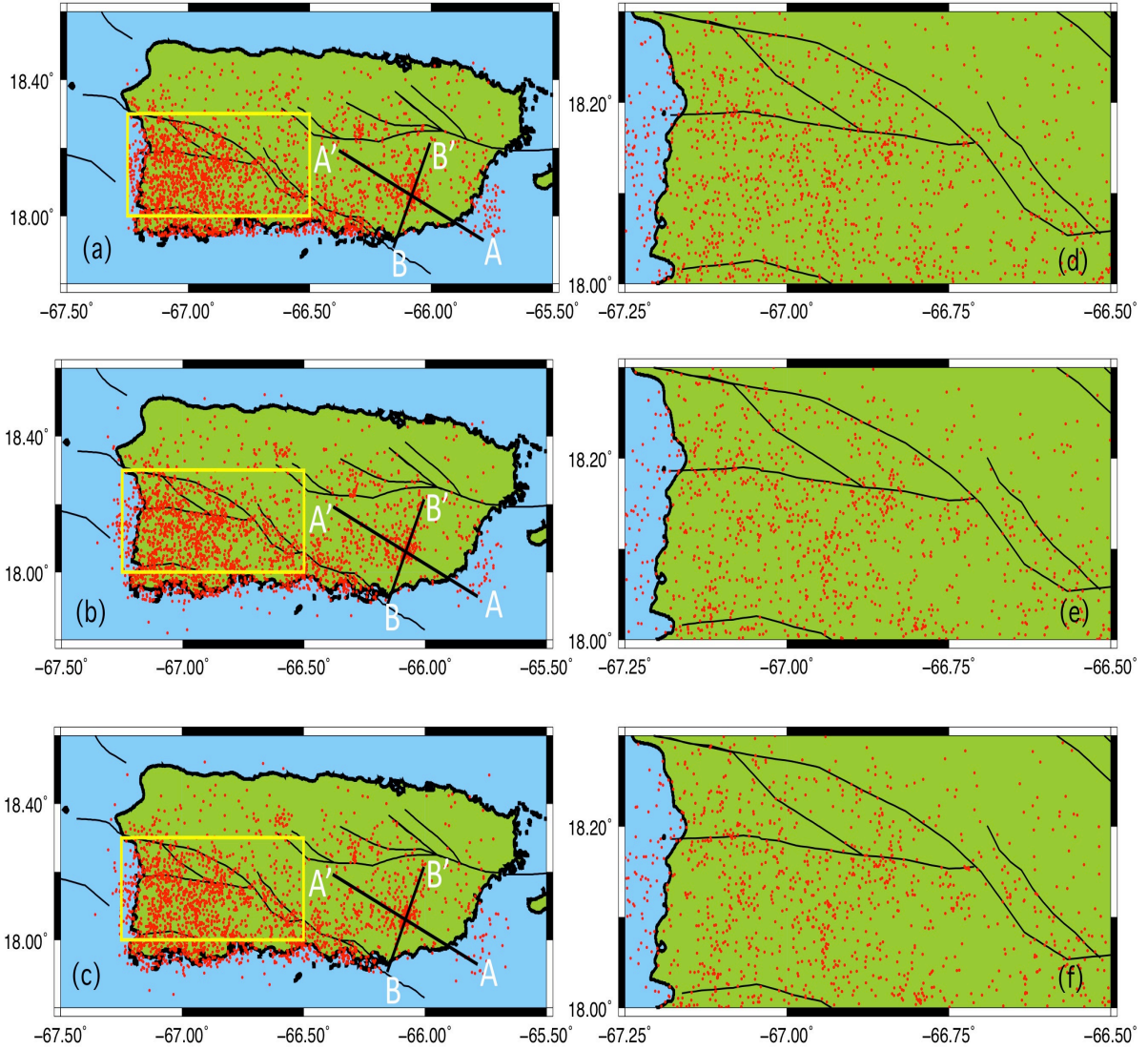


Figure 7. The left three panels are the map views of event locations from the PRSN catalog (a), relocations using the PRSN 1-D velocity model (b), and relocations with “minimum” 1-D velocity model (c). The right panels are close-up views of southwestern region denoted by yellow rectangles in left panels.

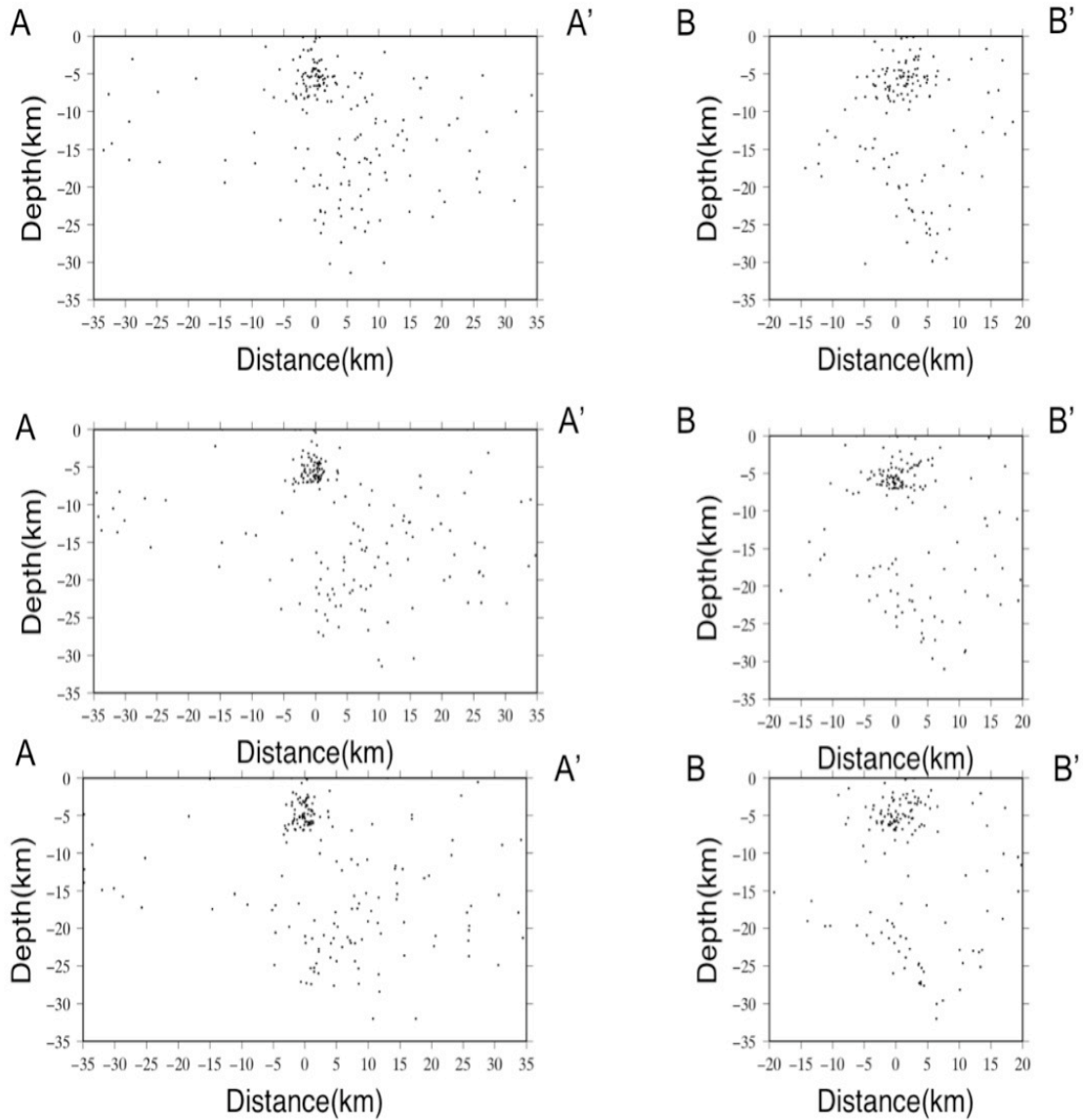


Figure 8. The top panels are the cross sections of PRSN catalog along the profiles AA' and BB'. The middle ones are cross sections of relocated events with the PRSN 1-D velocity model. The bottom cross sections are events relocated with the “minimum” 1-D velocity model. Earthquakes that fall within 5 km on either side of profile lines are plotted.

3D TOMOGRAPHY

To apply the FFM method, the first stage was to select a specific set of data, due to the complexity in the computations and to calibrate the software, we initiated with a subset of data (Table 1). All the events were selected inside the network and with depths above the known Moho interface, it was necessary to re-read all the secondary phases as that information is not included in the raw PRSN Catalogue (Figure 9). The initial velocity model was a composite ak135 including the PRSN upper layers.

No	PRSN ID	Latitude	Longitude	Depth (Km)	Magnitude
1	20060213204153	18.293	292.805	5.0	3.3
2	20070103002158	18.229	294.00	7.8	3.3
3	20070508082114	18.121	292.915	7.0	3.15
4	20071116100151	18.257	293.712	7.8	3.07
5	20071119083818	18.129	293.436	17.8	3.07
6	20081223024548	18.085	293.782	13.7	2.85
7	20081231040602	18.408	293.088	13.5	2.51
8	20090430063913	18.381	292.928	19.5	2.68
9	20091012203334	18.147	294.175	12.61	3.0
10	20091119044920	18.312	293.906	13.6	2.78

Table 1. Summary of the events used in the tomography computations.

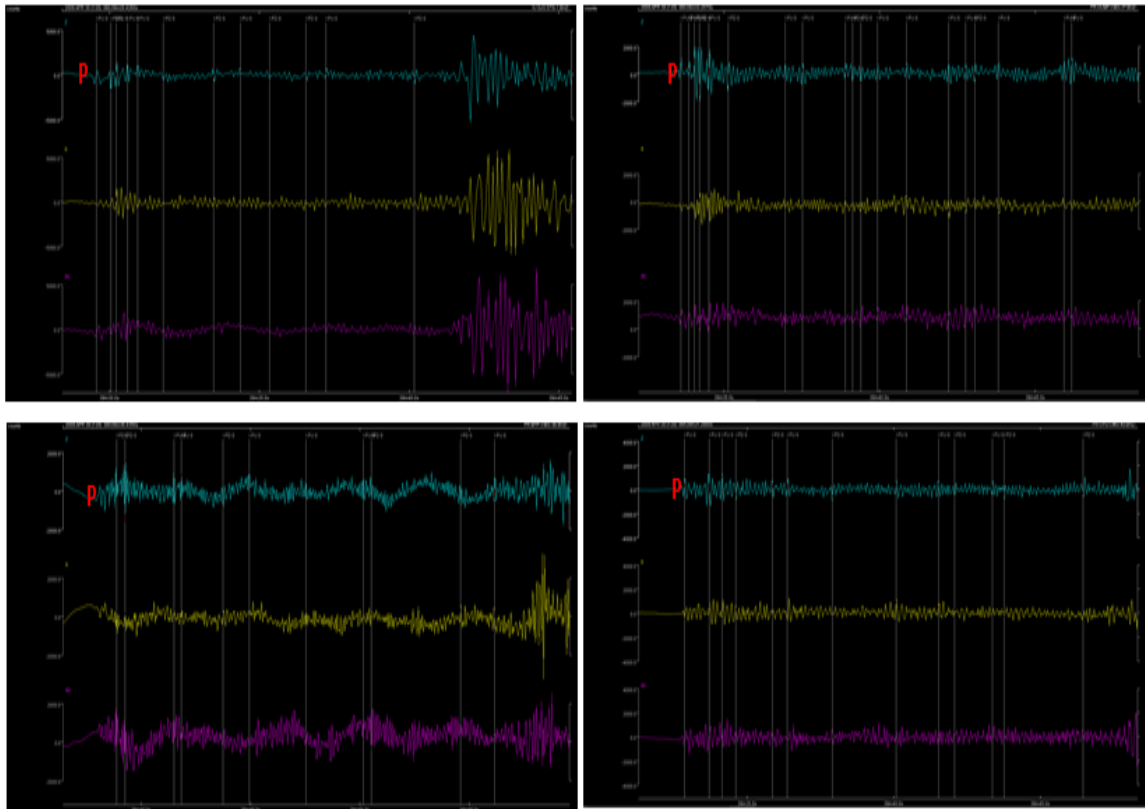
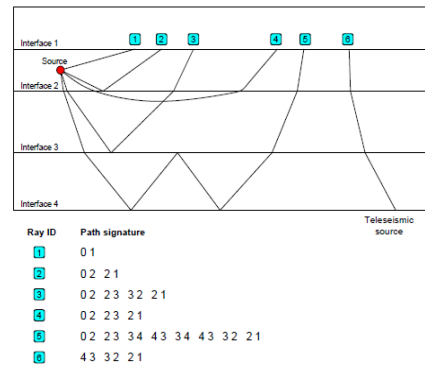


Figure 9. Event 20090430063913, station name is stamped in the up-right side of the waveform.

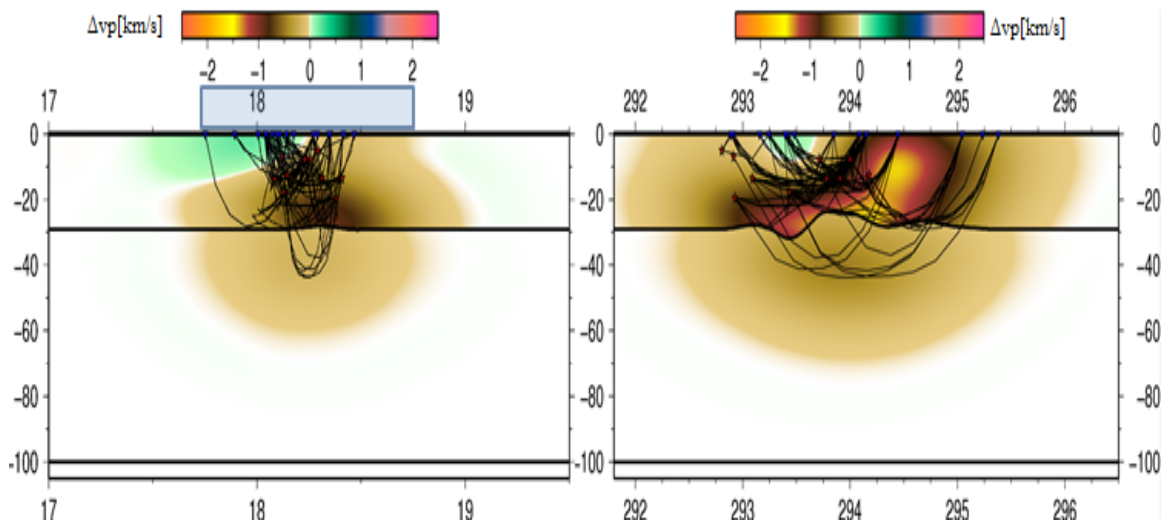
This initial schema consisted of a spatial grid of 31X41X41 (rad, lon, lat) or 52111 nodes. The phases were selected using the rule in the adjacent figure. A complex collection of 8 multiple arrivals tracked through the structure is shown in the figure between a single source and receiver, see the path 5. The most complex of these phases comprises N reflections and M transmissions. As more complex the layered model, more complex the nature of the velocity distribution.



The obtained 3D tomographic imaging scheme is used to construct a preliminary image of the lithosphere beneath Puerto Rico. The 3D model is parameterized using 52111 velocity nodes (approximately 7 km separation in each dimension), and six iterations of a 10-D subspace inversion method are used to minimize the objective function.

The pattern of variation (%) from the input velocity (V_p anomalies) is presented in the Figures 10. In particular, a strong negative velocity anomaly is identified towards the Virgin Islands (as observed in figure 3). One prominent upper mantle structure is a north-south dipping zone of higher velocity just beneath the south-western part of Puerto Rico, which becomes more diffuse at deep changing to negative at 20 km. Beneath the central south-east region of Puerto Rico, there is a broad region of shallow Moho which is overlain by a zone of lower velocity.

These 3D images are the first tomographic images for Puerto Rico, it is clear that more data must be used in the analysis and more detailed ray paths must be included. As outlined above, our new imaging results retain most of the basic features that are present in the station corrections plot. An unknown point is the low Moho depth to the south-east Puerto Rico.



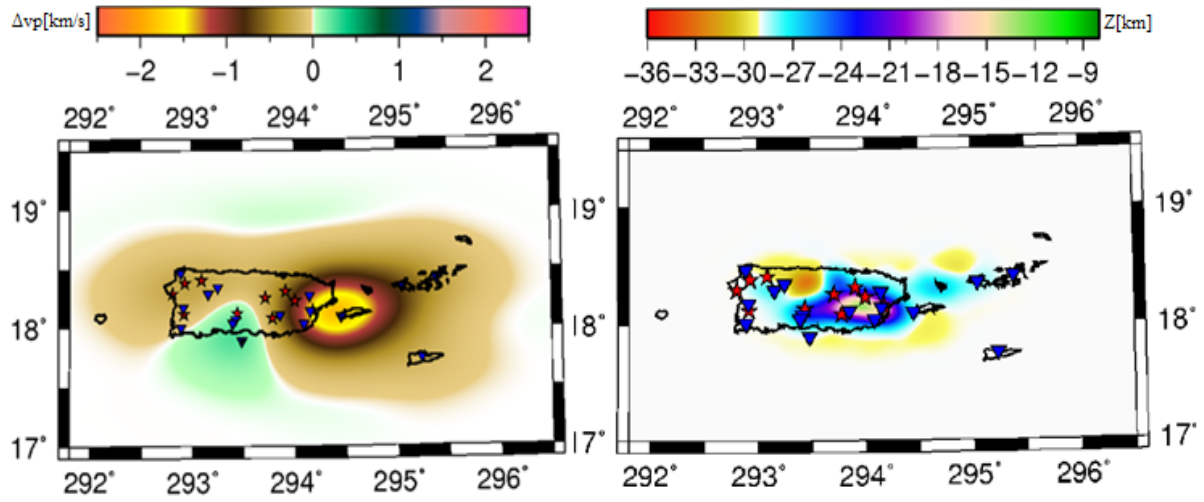


Figure 10. 3D imaging results from the FMTOMO inversion of local data for velocity anomalies and Moho structure of the lithosphere and upper crust beneath Puerto Rico. (Up-left) N-S view, (Up-right) E-W view, (Bottom-left) plain velocity anomaly view and (Bottom-right) Moho variability with depth. Red stars denote sources and blue inverted triangles denote receivers.

REFERENCES

- Census data for Puerto Rico, 2000. <http://www.census.gov/census2000/states/pr.html>
- Clinton, J., Cua, G., Huerfano, V., von Hillebrandt-Andrade, C., and Martinez-Cruzado, K. (2007). The current state of seismic monitoring in Puerto Rico. *Seismological Research Letters*, 77, 532-543.
- Efron, B., and G. Gong, (1983). A leisurely look at the bootstrap, the jackknife and cross-validation, *Am. Statist.*, 37, 36–48.
- Grindlay, N. R., M. Hearne, and P. Mann (2005). High risk of tsunami in the Northern Caribbean: Research focuses on active plate boundary faults and potential submarine landslides, *Eos, Transactions of the American Geophysical Union*, 86, 121.
- Grindlay, N., P. Mann, J. Dolan, and J. P. van Gestel (2005). Neotectonics and subsidence of the northern Puerto Rico–Virgin Islands margin in response to the oblique subduction of high-standing ridges. In *Active Tectonics and Seismic Hazards of Puerto Rico, the Virgin Islands, and Offshore Areas*, ed. P. Mann, Geological Society of America Special Paper 385, 31–60.
- Huérffano, V. (2003). Susceptibilidad de Puerto Rico ante el efecto de maremotos locales, PhD Thesis, Univ. of Puerto Rico-Mayagüez, Marine Sciences Department.
- Huérffano, V., and K. Bataille (1994). Crustal structure and stress regime near Puerto Rico, *PRSN Bulletin: Preliminary Locations of Earthquakes Recorded near Puerto Rico, Jan–Dec 1994*, 15–19.
- Huérffano, V., von Hillebrandt, C., and Baez-Sanchez, G., (2005), Microseismic Activity Reveals Two Stress Regimes in Southwestern Puerto Rico, In *Active Tectonics and Seismic Hazards of Puerto Rico, the Virgin Islands, and Offshore Areas*, ed. P. Mann, Geological Society of America Special Paper 385, 81-101.
- Kissling, E., W. L. Ellsworth, D. Eberhart-Phillips, and U. Kradolfer, (1994). Initial reference models in local earthquake tomography, *J. Geophys. Res.*, 99, 19,635–19,646.
- Klein, F. W. (2002). *User's Guide to HYPOINVERSE-2000, a Fortran Program to Solve for Earthquake Locations and Magnitudes*, USGS Open File Report 02-171, Version 1.0.
- Lin, G., and P. Shearer, (2005) Tests of relative earthquake location techniques using synthetic data, *J. Geophys. Res.*, 110, B04,304, doi:10.1029/2004JB003,380.

- Lin, G., and P. M. Shearer, (2006). The COMLOC earthquake location package, *Seismol. Res. Lett.*, 77, 440–444, 2006.
- Mendoza C., and V. Huérfino (2005). Earthquake location accuracy in the Puerto Rico Virgin Islands region, *Seismological Research Letters* 76, 356–363.
- Mueller, C., A. D. Frankel, M. D. Petersen, and E. V. Leyendecker (2003). *Documentation for 2003 USGS Seismic Hazard Maps for Puerto Rico and the U.S. Virgin Islands*, http://earthquake.usgs.gov/hazmaps/products_data/Puerto-RicoVI/prvi2003doc.html
- Prentice, C. S., P. Mann, and G. Burr (2000). Prehistoric earthquakes associated with a Late Quaternary fault in the Lajas Valley, southwestern Puerto Rico, *Eos, Transactions of the American Geophysical Union* 81, F1182 (abstract).
- Prentice, C. S., and P. Mann (2005). Paleoseismic study of the South Lajas fault: First documentation of an onshore Holocene fault in Puerto Rico. In *Active Tectonics and Seismic Hazards of Puerto Rico, the Virgin Islands, and Offshore Areas*, ed. P. Mann, Geological Society of America Special Paper 385, 215–222.
- Puerto Rico Seismic Network (PRSN). On line Seismic Catalogue, <http://prsn.uprm.edu>
- Rawlinson, N., and Sambridge, M., (2005), The fast marching method: an effective tool for tomographic imaging and tracking multiple phases in complex layered media: *Exploration Geophysics*, 36, 341–350.
- Rawlinson, N., Kennett, B. L. N., Heintz, M., (2006a). Insights into the structure of the upper mantle beneath the murray basin from 3-d teleseismic tomography. *Australian Journal of Earth Sciences* 53, 595–604.
- Rawlinson, N., Reading, A. M., Kennett, B. L. N., (2006b). Lithospheric structure of tasmania from a novel form of teleseismic tomography. *J. Geophys. Res.* 111, doi:10.1029/2005JB003803.
- Rawlinson, N., Hauser, J., and Sambridge, M., (2007). Seismic ray tracing and wavefront tracking in laterally heterogeneous media Research School of Earth Sciences, *Australian National University*, Canberra ACT 0200, Australia.
- Rawlinson, N., Pozgay, S. and Fishwick, S. (2010). Seismic tomography: A window into deep Earth. *Phys. Earth Planet. Inter.* 178, 101-135.
- Richards-Dinger, K. B., and P. M. Shearer, (2000) Earthquake locations in southern California obtained using source-specific station terms, *J. Geophys. Res.*, 105, 10,939–10,960.
- Sethian, J.A., and Popovici, A.M., (1999), 3-D travelttime computation using the fast marching method: *Geophysics*, 64, 516–523.

ten Brink, U. S., and J. Lin (2004). Stress interaction between subduction earthquakes and forearc strike-slip faults: Modeling and application to the northern Caribbean plate boundary, *Journal of Geophysical Research* 109, B12310.

BIBLIOGRAPHY

Zhang, Q, G. Lin, A. M. Lopez-Venegas, V. A. Huerfano, and L. Soto-Cordero, Earthquake relocations and location error estimates in the Puerto Rico Island, Abstract S21B-2030 presented at 2010 Fall Meeting, *AGU*, San Francisco, Calif., 13-17 Dec.

Huerfano, V. A., A. M., Lopez-Venegas, L. Castillo, G. Baez-Sanchez, L. Soto-Cordero, G. Lin, and Q. Zhang, Improving three dimensional velocity model for Puerto Rico-Virgin Islands for rapid earthquake relocations, Abstract S21B-2031 presented at 2010 Fall Meeting, *AGU*, San Francisco, Calif., 13-17 Dec.